



## Article

# Spatial and Temporal Analyses of Vegetation Changes at Multiple Time Scales in the Qilian Mountains

Lifeng Zhang<sup>1,2,3</sup>, Haowen Yan<sup>1,2,3</sup>, Lisha Qiu<sup>1,2,3</sup>, Shengpeng Cao<sup>1,2,3</sup>, Yi He<sup>1,2,3,\*</sup> and Guojin Pang<sup>1,2,3</sup>

<sup>1</sup> Faculty of Geomatics, Lanzhou Jiaotong University, Lanzhou 730070, China; zhanglf@mail.lzjtu.cn (L.Z.); yanhw@mail.lzjtu.cn (H.Y.); lisa\_qiu@nefu.edu.cn (L.Q.); 11200833@stu.lzjtu.edu.cn (S.C.); panggj@mail.lzjtu.cn (G.P.)

<sup>2</sup> National-Local Joint Engineering Research Center of Technologies and Applications for National Geographic State Monitoring, Lanzhou 730070, China

<sup>3</sup> Gansu Provincial Engineering Laboratory for National Geographic State Monitoring, Lanzhou 730070, China

\* Correspondence: heyi@mail.lzjtu.cn

**Abstract:** The Qilian Mountains (QLMs), an important ecological protective barrier and major water resource connotation area in the Hexi Corridor region, have an important impact on ecological security in western China due to their ecological changes. However, most existing studies have investigated vegetation changes and their main driving forces in the QLMs on the basis of a single scale. Thus, the interactions among multiple environmental factors in the QLMs are still unclear. This study was based on normalised difference vegetation index (NDVI) data from 2000 to 2019. We systematically analysed the spatial and temporal characteristics of the QLMs at multiple time scales using trend analysis, ensemble empirical mode decomposition, Geodetector, and correlation analysis methods. At different time scales under single-factor and multi-factor interactions, we examined the mechanisms of the vegetation changes and their drivers. Our results showed that the vegetation in the QLMs showed a trend of overall improvement in 2000–2019, at a rate of  $0.88 \times 10^{-3}$ , mainly in the central western regions. The NDVI in the QLMs showed a short change cycle of 3 and 5 years and a long-term trend. Sunshine time and wind speed were the main drivers of the vegetation variation in the QLMs, followed by temperature. Precipitation affected the vegetation spatial variation within a certain altitude range. However, temperature and precipitation had stronger explanatory powers for the vegetation variation in the western QLMs than in the eastern part. Their interaction was the dominant factor in the regional differences in vegetation. The responses of the NDVI to temperature and precipitation were stronger in the long time series. The main drivers of vegetation variation were land surface temperature and precipitation in the east and temperature and evapotranspiration in the west. Precipitation was the main driver of vegetation growth in the northern and southwestern QLMs on both the short- and long-term scales. Vegetation changes were more significantly influenced by short-term temperature changes in the east but by a combination of temperature and precipitation in most parts of the QLMs on a 5-year time scale.

**Keywords:** vegetation change; driver; EEMD; Geodetector; QLMs



**Citation:** Zhang, L.; Yan, H.; Qiu, L.; Cao, S.; He, Y.; Pang, G. Spatial and Temporal Analyses of Vegetation Changes at Multiple Time Scales in the Qilian Mountains. *Remote Sens.* **2021**, *13*, 5046. <https://doi.org/10.3390/rs13245046>

Academic Editors: Inkyu Sa, Marija Popović and Ho Seok Ahn

Received: 29 September 2021

Accepted: 9 December 2021

Published: 12 December 2021

**Publisher's Note:** MDPI stays neutral with regard to jurisdictional claims in published maps and institutional affiliations.



**Copyright:** © 2021 by the authors. Licensee MDPI, Basel, Switzerland. This article is an open access article distributed under the terms and conditions of the Creative Commons Attribution (CC BY) license (<https://creativecommons.org/licenses/by/4.0/>).

## 1. Introduction

The ecological environment is an important barrier to human survival on earth. In recent years, with the active promotion of urbanisation and rapid industrialisation, the ecological environment has been changing drastically. Protection of the ecological environment and its rational exploitation have become increasingly important in the context of sustainable development [1]. Surface vegetation is a sensitive indicator of environmental change that can directly respond to the overall ecological environmental situation [2] and then provide reliable information for ecological environment construction and protection. As an effective index for characterising surface vegetation changes, the normalised difference vegetation index (NDVI) can fully reveal the spatial pattern of vegetation cover

and its heterogeneity and has been widely used in monitoring vegetation productivity, drought, desertification, and ecological environment [3–5]. Many human activities such as deforestation, overgrazing, and mineral development have adverse effects on the ecological environment. Thus, the use of the NDVI as an indicator to account for and evaluate regional vegetation cover changes and examine the driving factors affecting vegetation changes is of great practical significance to the improvement and restoration of the local ecological environment. The NDVI is also useful for reconciling the contradiction between socio-economic development and ecological environmental protection.

In recent years, along with the rapid development of remote sensing technology with good application prospects, ecological environment monitoring based on remote sensing technology has become an indispensable technical tool [6]. Satellite-based NDVI can accurately reflect the density and growth of vegetation cover and is the most commonly used indicator for characterising the status of surface vegetation [7]. On this basis, many scholars have conducted fruitful studies on vegetation changes on the global and regional scales by using NDVI datasets [8–10]. At the global level, global vegetation cover has increased since 1980, which is mainly attributed to improved climatic conditions and elevated CO<sub>2</sub> concentrations [11]. Since 1990, increased brownout trends have slowed down the growth rate of the global average of the NDVI. Since 2000, global vegetation has been at risk of shifting from long-term increases to degradation as the climate continues to warm [12]. At regional scales, vegetation NDVI trends vary and are associated with multiple factors, so quantifying the drivers and the interaction of multiple factors is key in the research on the mechanisms of vegetation changes.

Furthermore, the NDVI in China has continued to increase over the past 30 years, with a clear spatial increase in North China and an overall decrease in South China. The NDVI in the arid and semi-arid regions of northwest China increased significantly in spring, whereas that in northern and northeastern China showed an increasing trend in summer and autumn [13]. In the case of northwest China, which has a special topography, the NDVI of vegetation showed an overall increasing trend, and the vegetation changes showed a significant regional variability. Studies have shown that the NDVI of the vegetation changes in northwest China is weakly correlated with temperature as a whole, whereas that in arid and semi-arid areas is negatively correlated with temperature. The change in the NDVI in different vegetation types has spatial and temporal variabilities, and the correlation with factors such as temperature and precipitation also had notable differences [14].

As a watershed between the Qinghai-Tibet Plateau and the northern inland desert, the Qilian Mountains (QLMs) are an important ecological barrier in northwest China and a major water resource culmination area in the Hexi Corridor region. Their ecological changes not only affect the local socioeconomic and ecological environments but also play an extremely important regulatory role in the ecological security of western China [15]. The QLMs are also a fragile ecological zone in northwest China, which is extremely sensitive to climate change and human activities owing to its highly unstable natural conditions [16]. Therefore, the vegetation cover changes reflected by the NDVI in the QLMs are significantly related to the spatial heterogeneity of climate factors. The changes in vegetation growth and regional ecological structure within a certain time scale are inevitably influenced by abrupt changes in climate factors.

Vegetation change and its drivers are characterised by multiple time scales, and their relationships are also scale dependent [17]. However, most existing studies on the QLMs have used a single time scale and spatial scale to analyse vegetation change patterns. While most long-term changes in climate variables exhibit non-linear and non-smooth complex processes with different time scales and periodic oscillations [18], a single time scale cannot accurately reflect the interactions between vegetation and climate transformations. By focusing on region-wide or larger-scale vegetation characterisations, reflecting on the comprehensive microscopic characteristics of vegetation changes and their patterns is difficult [19]. Moreover, a previous study on vegetation and driver interrelationships in the QLMs did not consider the complex relationships between geographic variables

and lacked a quantitative evaluation of the interaction between two or more drivers [20]. Geodetector can assess the main drivers of regional vegetation and the interaction between variables from the perspective of spatial heterogeneity and stratification [21,22], which can be introduced in studies on the drivers of vegetation change in QLMs.

In view of this, on the basis of the MODIS and GIMMS NDVI data of the QLMs in the periods 2000–2019 and 1982–2006, this study combined various meteorological data, digital elevation models (DEMs), land surface temperatures (LSTs), and evapotranspiration (ET). The linear trend and ensemble empirical mode decomposition (EEMD) methods were used to analyse the evolution pattern of vegetation in the QLMs on multiple time scales. Geodetector was applied to determine the main control factors of vegetation change and the interaction between the factors. The quantitative relationships between vegetation change and the driving factors were examined to provide technical support for ecological restoration, conservation, and sustainable development of the QLMs and a reference for the study of vegetation cover change in the same types of areas.

## 2. Study Area and Data

### 2.1. Study Area

The QLMs are the dividing line between the three major plateaus, namely Loess, Mengxin, and Qinghai-Tibet, in the arid and semi-arid regions of inland northwest China [23]. The geographical coordinates lie between  $93^{\circ}30'–103^{\circ}$  E and  $36^{\circ}30'–39^{\circ}30'$  N. The total length is around 1000 km, and the width is around 300 km [15,24]. The QLMs extend from Wushaoling in the east to the Dangjinshan Pass and Altun Mountain in the west and are bounded by the Hexi Corridor in the north and adjacent to the Qaidam Basin in the south. The terrain is high in the southwest and low in the northeast, consisting of several northwest-to-southeast-trending mountain ranges and wide valleys, with peaks mostly higher than 4000 m in elevation. Qinghai Lake is its largest lake (Figure 1). The QLMs belong to the mid-latitude northern temperate zone, which is a typical continental climate of the plateau.

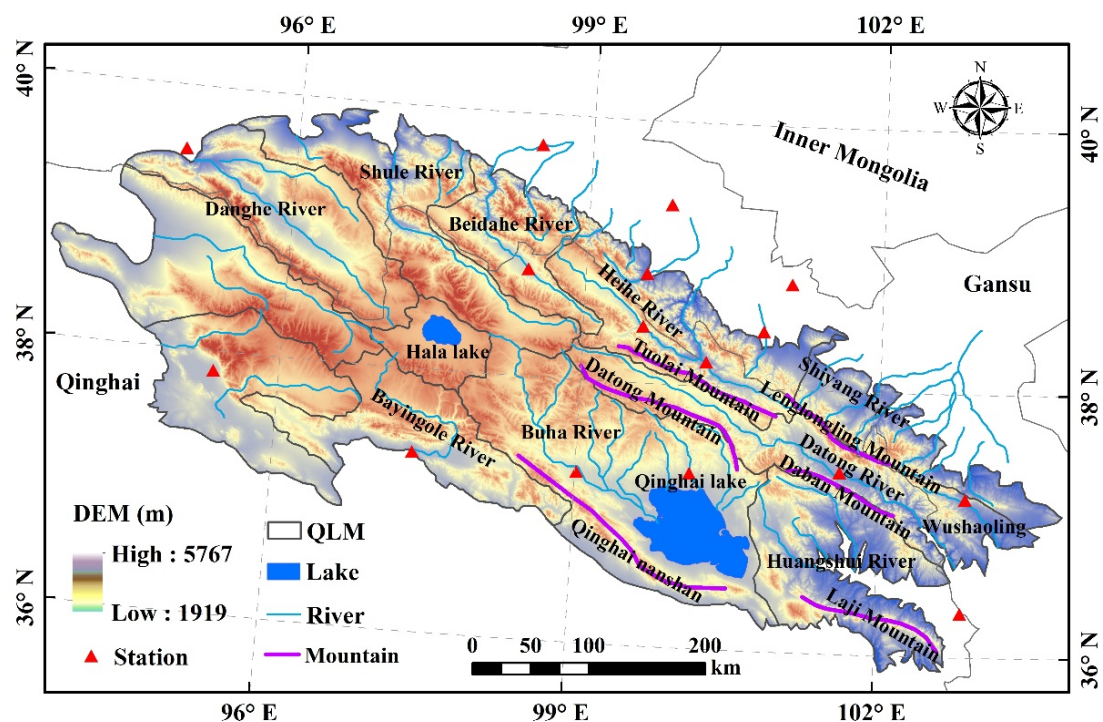


Figure 1. The geographical location of QLMs.

Owing to the influence of atmospheric circulation and high altitude, the water and heat conditions in the QLMs vary greatly from east to west, with an average annual temperature of around 0.6 °C and annual precipitation of around 400 mm, decreasing from east to west. As a result of the special topography and abundant water vapour overhead, precipitation is higher in the mountains by around 400–700 mm [25–27]. The QLMs water system is dominated by glacial meltwater recharge and mountain precipitation. The distribution of vegetation in the area is affected by the southeast monsoon and the redistribution of water and heat conditions and terrain patterns. Thus, the QLMs show unique vertical zonation characteristics, with semi-desert grasslands, mountain desertification grasslands, mountain forest grasslands, alpine scrub meadows, alpine meadows, and alpine sparse meadows distributed from low to high altitudes [28]. Owing to complex topographic and climatic conditions, the natural ecosystems in the region are fragile and sensitive to climate change. The changing characteristics of vegetation in the QLMs have attracted great attention in China.

## 2.2. Data

Vegetation data were obtained from MOD13Q1 data, with a temporal resolution of 16 d and a spatial resolution of 250 m from NASA for the period 2000–2019 (<https://ladsweb.modaps.eosdis.nasa.gov/>, accessed on 29 September 2021). The downloaded MODIS NDVI data were pre-processed using the MODIS Reprojection Tool (MRT) for stitching, projection conversion, and cropping. The monthly data were maximally synthesised using the maximum value compound (MVC) method to eliminate the interference of clouds, atmosphere, and solar altitude angle [16]. An NDVI of 0.1 or more is generally considered to indicate vegetation cover. For this reason, in this study, we cropped out areas without vegetation cover, such as bare soil, gobi deserts, water bodies, snow, and ice, with NDVI values < 0.1 [29]. Owing to the short time series of the MODIS data, the GIMMS NDVI and MODIS NDVI data were partially fused to extend the time series for the examination of the cyclic relationship with the NDVI.

In this study, the GIMMS NDVI dataset, with a resolution of 8 km and temporal resolution of 15 d, for the period 1982–2006 was selected from the National Oceanic and Atmospheric Administration land dataset [18]. The GIMMS NDVI data were obtained from the WGS84 dataset and pre-processed with radiometric correction, geometric refinement correction, atmospheric correction, bad-line removal, cloud removal, and so forth. The data quality was good and had a long time series, which is widely used in current large-scale vegetation change studies [30]. The LST and ET data were also obtained from the MOD11A2 and MOD16A2 datasets provided by NASA (<https://ladsweb.modaps.eosdis.nasa.gov/>, accessed on 29 September 2021), which were stitched, reprojected, cropped, and synthesised with maximum values. MVC was used to support the discussion of the correlation between the vegetation changes and the LST and ET in the QLMs.

The meteorological data selected for this study were obtained from the China Meteorological Science Data Sharing Service (<http://data.cma.cn/>, accessed on 29 September 2021). These include the monthly mean temperature, precipitation, mean wind speed, sunshine hours, and relative humidity data of five meteorological factors from 2000 to 2019. These data cover 16 meteorological stations in the QLMs and surrounding areas and were used to discuss the main drivers of vegetation change in the QLMs.

The DEM data were obtained from the geospatial data cloud (<http://www.gscloud.cn/>, accessed on 29 September 2021). The DEM data were obtained from the SRTM DEM data, with a spatial resolution of 90 m, an absolute horizontal error of 20 m, and a vertical error of 16 m (90% confidence level) [31]. The projection was transformed and resampled to match the geographic coordinates and resolution to the vegetation NDVI data.

### 3. Methods

#### 3.1. Unary Linear Regression Trend Method

In this study, the linear trend method was used to simulate the vegetation cover change trend in the QLMs from 2000 to 2019. In this method, the rate of vegetation change was calculated using the following formula:

$$\Theta_{slope} = \frac{n \times \sum_{i=1}^n (i \times NDVI_i) - \sum_{i=1}^n i \times \sum_{i=1}^n NDVI_i}{n \times \sum_{i=1}^n i^2 - (\sum_{i=1}^n i)^2} \quad (1)$$

In Equation (1),  $n$  is the cumulative number of years in the monitoring period,  $NDVI_i$  is the NDVI in year  $i$ , and  $\theta_{slope}$  is the change rate.  $\theta_{slope} > 0$  indicates an increasing NDVI trend over  $n$  years, and conversely,  $\theta_{slope} < 0$  indicates a decreasing NDVI trend [32]. The F test was used to determine the significance level of the vegetation change trends. On the basis of the range of changes in the slope of the trend line, highly significant improvement ( $\theta_{slope} > 0$ ,  $p \leq 0.01$ ), significant improvement ( $\theta_{slope} > 0$ ,  $0.01 < p \leq 0.05$ ), insignificant change ( $p > 0.05$ ), significant decrease ( $\theta_{slope} < 0$ ,  $0.01 < p \leq 0.05$ ), and highly significant decrease ( $\theta_{slope} < 0$ ,  $p \leq 0.01$ ) were observed in the five change intervals [33].

#### 3.2. NDVI Data Fusion

In this study, MODIS NDVI data from 2000 to 2019 and the reconstructed GIMMS NDVI dataset from 1982 to 2006 were selected to remove as much noise as possible and reduce the impact on the effectiveness of surface vegetation monitoring. NDVI reconstruction methods can be broadly classified into four categories [31]: (1) Savitzky-Golay filtering method; (2) Fourier fitting method; (3) threshold methods such as standard deviation and best exponential slope extraction; and (4) asymmetric function fitting methods such as asymmetric Gaussian function fitting and weighted least squares linear regression. The literature analysis revealed that the asymmetric Gaussian function fitting method had better results. Therefore, in this study, an asymmetric Gaussian function was used to reduce noise in the MODIS NDVI series, and the NDVI values of the study area were calculated. The asymmetric Gaussian function was first fitted to the data points around the extremes by using the local Gaussian function. Then, the adjacent local functions obtained from the fitting were spliced to form the global fitting function [30,34]. The local function is expressed as:

$$f(t) = c_1 + c_2 \times g(t, x_1, x_2, x_3, x_4, x_5) \quad (2)$$

where  $c_1$  and  $c_2$  are the coefficients of the basic function, which determine the baseline and amplitude of the local fitting function, respectively, and the function  $g$  is a Gaussian function with the expression

$$g(t, x_1, x_2, x_3, x_4, x_5) = \begin{cases} \exp\left[-\left(\frac{t-x_1}{x_2}\right)^{x_3}\right] & t \geq x_1 \\ \exp\left[-\left(\frac{x_1-t}{x_4}\right)^{x_5}\right] & t < x_1 \end{cases} \quad (3)$$

where  $x_1$  is the time scale at which the extreme value is located;  $x_2$  and  $x_3$  are the coefficients determining the width and flatness of the Gaussian right-hand function, respectively; and  $x_4$  and  $x_5$  are the coefficients determining the width and flatness of the left-hand function, respectively.

The global formula derived from the local formula is

$$F(t) = \begin{cases} a(t) \times f_1(t) + [1 - a(t)] \times f_2(t) & t_1 < t < t_2 \\ b(t) \times f_2(t) + [1 - b(t)] \times f_3(t) & t_2 < t < t_3 \end{cases} \quad (4)$$

where  $f_1(t)$  is the local fit function around the left minimum,  $f_3(t)$  is the local fit function around the right minimum, and  $f_2(t)$  is the local fit function around the middle maximum.

$a(t)$  and  $b(t)$  are the normalised distance factors of  $t$ , respectively, ranging from 0 to 1. Figure 2 shows the NDVI fitting effect based on the asymmetric Gaussian function.

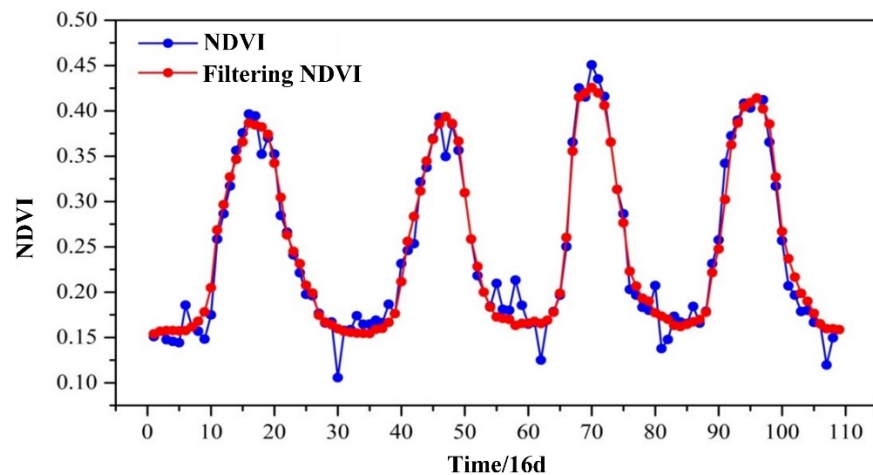


**Figure 2.** NDVI fitting effect based on asymmetric Gaussian function.

### 3.3. Ensemble Empirical Mode Decomposition

Empirical mode decomposition (EMD) is a signal time-frequency processing method. It is based on the Hilbert–Huang transform, which can decompose a signal into a finite number of intrinsic mode function (IMF) components containing local features of the original signal at different time scales and a trend component according to the characteristics of the signal itself [35,36]. EEMD is an improved empirical mode decomposition method [37]. EEMD inherits the adaptive characteristics of EMD and effectively solves the modal mixing problem by introducing auxiliary white noise [18]. In this study, the EEMD model was used to analyse long-term vegetation periodicity.

The EEMD decomposition steps are as follows:

1. Add a certain number ( $np$ ) of Gaussian white noise  $\omega_j(t)$  to the signal  $x(t)$  to obtain a large number of noisy new signals  $X_j(t)$ .

$$X_j(t) = x(t) + \omega_j(t) \quad (5)$$

$$j = 1, 2, \dots, np \quad (6)$$

2. Decompose the new signal  $X_j(t)$  by EMD method to obtain the IMF component ( $c_i$ ) and the trend term ( $r_n$ ):

$$X_j(t) = \sum_{i=1}^n c_{ij} + r_{nj} \quad (7)$$

where  $c_{ij}$  and  $r_{nj}$  denote the IMF component and trend term, respectively.

3. Repeat the above steps for  $np$  times; each time, a new white noise sequence with the same amplitude is added.
4. The IMFs and  $r_n$  obtained from each decomposition are pooled and averaged so that the added white noises cancel each other as follows.

$$c_i(t) = \frac{1}{np} \sum_{j=1}^{np} c_{ij}(t) \quad (8)$$

$$r_n = \frac{1}{np} \sum_{j=1}^{np} r_{nj}(t) \quad (9)$$

where  $c_i(t)$  is the  $i$ th IMF component obtained by decomposition of the initial signal, and  $r_n$  is the trend term.

The variation period of each IMF component is as follows:

$$T_k = \frac{N}{NP_k} \quad (10)$$

where  $N$  is the length of the IMF component and  $NP_k$  is the number of extreme value points of the  $k$ th IMF component.

The significance of IMF components at different time scales can be estimated by the variance contribution ratio, as follows:

$$S_i = \sum_{i=1}^k (c_i(t))^2 - \left( \sum_{i=1}^k c_i(t) \right)^2 \quad (11)$$

$$S = \frac{S_i}{\sum_{i=1}^{i-1} S_i} \times 100\% \quad (12)$$

where  $S_i$  is the variance of the  $i$ th component  $c_i(t)$  and  $S$  is the variance contribution of this component. The larger the value of  $S$ , the more volatile and important this component [35].

### 3.4. Geodetector

Geodetector is a statistical method proposed by Wang [38] that can quantitatively detect spatial dissimilarity and reveal the driving force. The core idea of the method is that if a factor has a spatially significant influence on the emergence of a phenomenon, then the factor should have similarities with the spatial distribution of the phenomenon. This method can detect the influence of a single factor and judge the strength of multi-factor interactions.

Geodetector consists of four detectors: variance and factor detection, interaction detection, risk area detection, and ecological detection. We used variance and factor detection, interaction detection, and ecological detection to analyse the quantitative relationship between vegetation change and the driving factors.

Variance and factor detection identifies the extent to which factor  $X$  explains the spatial divergence of an attribute  $Y$ . The value of  $q$  is measured in the range of  $[0,1]$ . The larger the value of  $q$ , the stronger the explanatory power of the independent variable  $X$  on attribute  $Y$ , and the weaker the opposite. The expressions are as follows:

$$q = 1 - \frac{SSW}{SST} \quad (13)$$

$$SSW = \int_{h=1}^L N_h \sigma_h^2 \quad (14)$$

$$SST = N\sigma^2 \quad (15)$$

where  $h = 1, \dots, L$ ;  $L$  is the stratification (Strata) of variable  $Y$  or factor  $X$ , classification or partition;  $N_h$  and  $N$  are the numbers of cells in stratum  $h$  and the whole area, respectively; and  $\sigma_h^2$  and  $\sigma^2$  are the variance of the  $Y$  values in stratum  $h$  and the whole area, respectively.  $SSW$  and  $SST$  are the sum of the within sum of the squares and total sum of the squares, respectively.

Interaction detection identifies interactions between different risk factors  $X_s$  and assesses the explanatory power of factors  $X_1$  and  $X_2$  when acting together to increase or decrease the explanatory power of the dependent variable  $Y$ . The assessment is performed by calculating the  $q$  values of  $X_1$  and  $X_2$  on  $Y$ ,  $q(X_1)$  and  $q(X_2)$ , respectively. Then, the  $q$  values when  $X_1$  and  $X_2$  interact,  $q(X_1 \cap X_2)$ , were calculated. Finally,  $q(X_1)$ ,  $q(X_2)$ , and  $q(X_1 \cap X_2)$  were compared. The relationship between the two factors can be divided into the following categories (Table 1):

**Table 1.** Types of interactions between two independent and dependent variables.

Judgment Basis	Interaction
$q(X1 \cap X2) < \text{Min}(q(X1), q(X2))$	Non-linear weakening
$\text{Min}(q(X1), q(X2)) < q(X1 \cap X2) < \text{Max}(q(X1), q(X2))$	Single-factor nonlinear attenuation
$q(X1 \cap X2) > \text{Max}(q(X1), q(X2))$	Two-factor enhancement
$q(X1 \cap X2) = q(X1) + q(X2)$	Independent
$q(X1 \cap X2) > q(X1) + q(X2)$	Non-linear enhancement

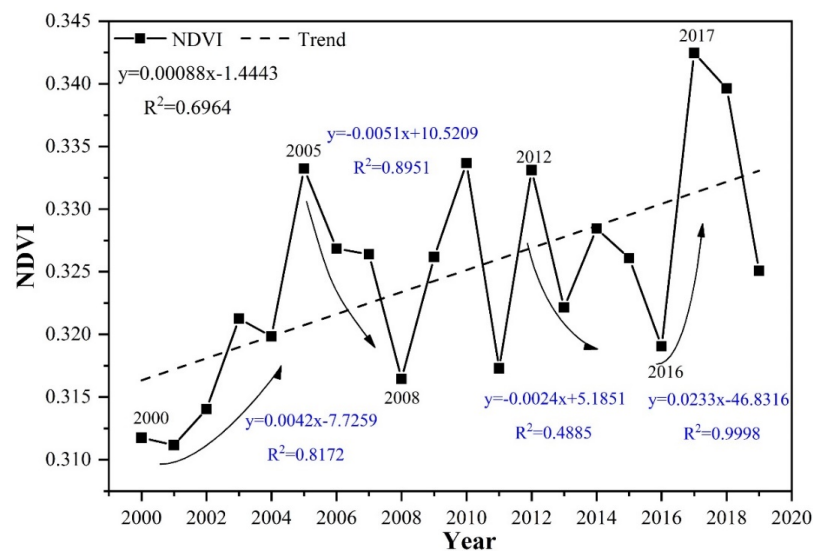
### 3.5. Correlation Analysis

We used a correlation analysis to study the relationship between NDVI and climate factors, mainly to study the degrees of correlation of NDVI to temperature and precipitation, and the correlation coefficient was within the range  $[-1, 1]$ . The larger the absolute value of the correlation coefficient, the higher the correlation between vegetation change and climate factors, and the smaller the absolute value of the correlation coefficient, the lower the correlation between the two [39].

## 4. Results

### 4.1. Spatial and Temporal Characteristics of the Vegetation Changes in the QLMs

In terms of time, the NDVI change rate in the QLMs during the growing season was  $0.88 \times 10^{-3}$  (Figure 3). The mean NDVI value in the QLMs during the growing season from 2000 to 2019 showed an upward trend of fluctuation, with the minimum (0.31) and maximum values (0.34) appearing in 2001 and 2017, respectively. From 2000 to 2005, the NDVI showed an upward trend, with a growth rate of  $4.20 \times 10^{-3}$ . From 2005 to 2008 and from 2012 to 2016, the NDVI showed a decreasing trend and reached the smallest value in 2008. From 2008 to 2012, the NDVI showed an upward trend of fluctuation and increased rapidly, with a growth rate of  $23.33 \times 10^{-3}$  from 2016 to 2017, reaching the maximum value in 2017.

**Figure 3.** Interannual trends in vegetation cover in the QLMs.

Spatially, the vegetation distribution in the QLMs showed obvious spatial differences and generally decreased from east to west (Figure 4). The high vegetation coverage areas were mainly concentrated in Wushaoling, Daban Mountain, Lenglongling Mountain, Qinghai Nanshan, and other typical grassland coverage areas in the east, with NDVI values ranging from 0.5 to 0.7, accounting for 17.53% of the total area. The vegetation coverage areas of Corridor Nanshan, Tuolai Mountain, Datong Mountain, and the northwest part

of Qinghai Lake were less than those of the high vegetation areas mentioned earlier, with NDVI values between 0.3 and 0.5.

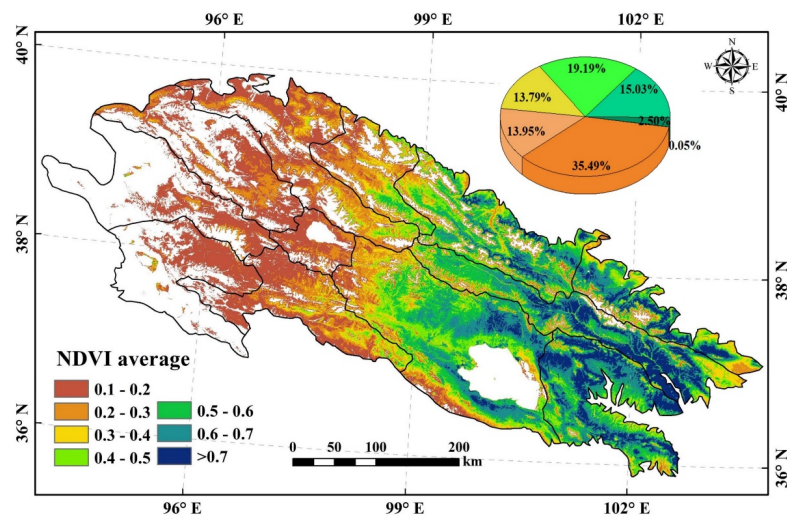


**Figure 4.** Spatial distribution characteristics of vegetation in the QLMs.

The spatial change rate of vegetation in the growing season was between  $-0.6$  and  $0.6$  (Figure 5a), indicating a significant growth trend. The regions with a change rate higher than  $0.2$  were mainly distributed on the north and south sides of the QLMs, including Buha River, Qinghai Nanshan, and both sides of Laji Mountains in the south and Lenglongling Mountain and Tuolai Mountain in the north. The regions with large negative change rates were mainly distributed in the middle and east of the study area, with change rates between  $-0.2$  and  $-0.6$ . The proportion of the area with a negative change rate between  $0.4$  and  $0.6$  was small, accounting for  $0.05\%$  of the area. The areas with a negative change rate between  $0.2$  and  $0.4$  were mainly distributed among the basins of the Datong River, Huangshui River, and Shiyang River.

In the west of the study area, the vegetation change rate was relatively low, mostly between  $-0.2$  and  $0.2$ . The areas with significant increases and decreases in vegetation coverage accounted for  $32.55\%$  and  $1.56\%$ , respectively (Figure 5b). The significant increase was roughly similar to the area spatial distribution of the change rate higher than  $0.2$ , which was distributed in the Buha River basin and both sides of the Laji Mountains. In the northwest of the study area, the vegetation change rates of the North and Shule River basins were not high but showed significant increase trends. The area of vegetation with an extremely significant increase accounted for  $19.45\%$ . Areas with significant vegetation degradation were distributed in the Datonghe River and Huangshui River basins. Vegetation degradation was obvious in the Huangshui River basin, accounting for  $0.51\%$  of the area. In summary, the NDVI value of the QLMs showed an overall improvement trend from 2000 to 2019, with a spatial distribution characteristic of higher NDVI in the northeast and lower NDVI in northwest. The vegetation improved significantly in the central and western regions, whereas the local vegetation degradation was significant in the eastern region of the QLMs.

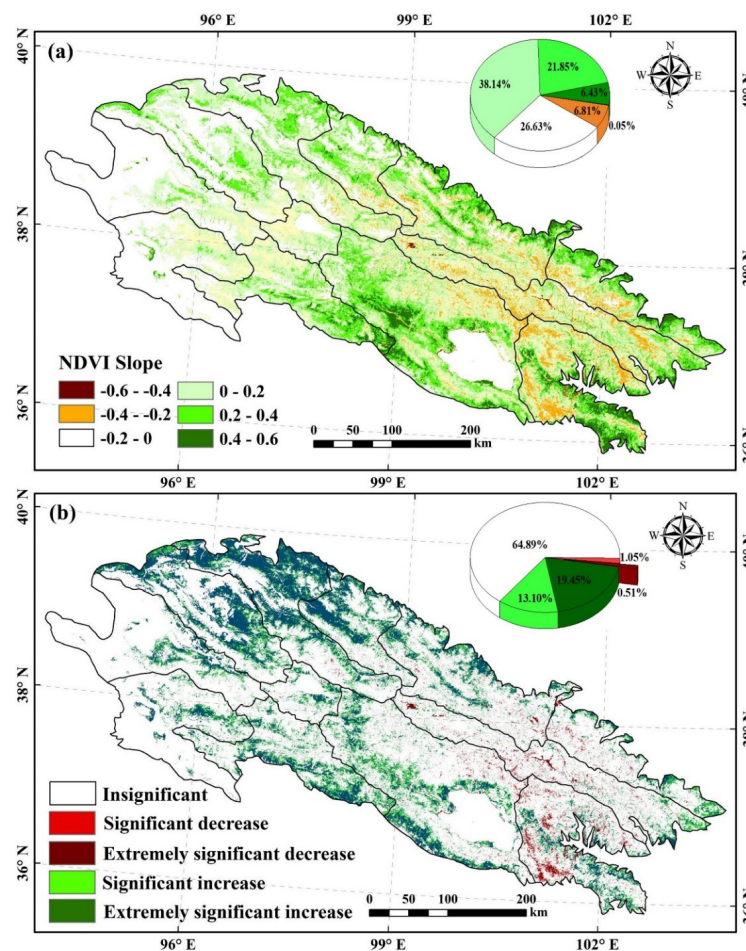


**Figure 5.** Spatial distribution of vegetation change rates (a) and trends (b) in the QLMs.

## 4.2. Vegetation Change Characteristics of the QLMs at Different Time Scales

### 4.2.1. Periodicity Analysis

The decomposition of EEMD should take into account the following factors: The data are greater than or equal to two extreme values. The characteristic time scale is defined by the time interval between the extreme values. If the data have no extreme values at all and contain only inflection points, they can be differentiated one or more times to reveal the extreme values. Each IMF must meet two conditions: In the entire data set, the numbers of extremes and zero crossings must be equal or not more than 1. The average value of the upper and lower envelopes determined by the maximum and minimum values in the signal is zero; that is, the upper and lower envelopes are locally symmetrical with respect to the zero axis. The average period of each IMF component can be obtained by dividing the number of peaks (local maximums) by the length of time. We extracted the IMF component of NDVI in the QLMs from 1982 to 2019 by using the EEMD method (Figure 6). Then, we calculated the oscillation period of each component and its corresponding variance contribution rate (Table 2) to reveal the cyclical characteristics of the NDVI change.

NDVI was decomposed into four IMF components with corresponding fluctuation cycles of 3, 5, 13, and 24 years (Figure 6). Among these components, IMF1 had the largest variance contribution rate (29.49%), followed by IMF2 (23.51%). The variance contribution rates of IMF3, IMF4, and the trend term Residue (RES) were 20.50%, 16.63%, and 9.87%, respectively (Table 2). The cycle detection of IMF1, IMF2, and IMF3 all passed the significance test of 95%, but the cycle change of IMF4 was not obvious. The trend term RES showed an upward trend, indicating that the overall NDVI value in the QLMs showed

an upward trend from 1982 to 2019. In summary, the NDVI in the QLMs mainly showed a 3- and 5-year cycle change and long-term growth trend.

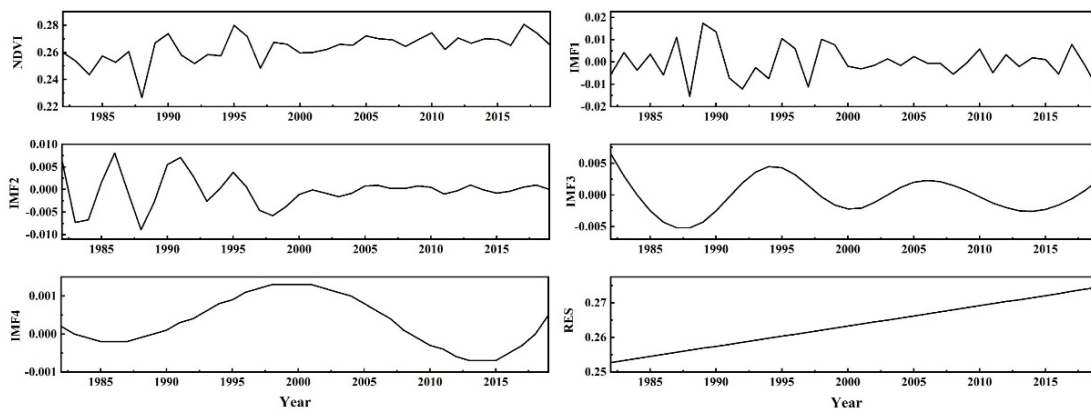


Figure 6. Trend decomposition of the NDVI series of QLMs vegetation based on EEMD model.

Table 2. Periods and variance contributions of the IMF components of the QLMs vegetation NDVI series.

	IMF1	IMF2	IMF3	IMF4	Trend Term (RES)
Periodicity	3	5	13	24	—
Variance contribution (%)	29.49	23.51	20.50	16.63	9.87

#### 4.2.2. Analysis of Vegetation Change at Multiple Time Scales

As shown in Figures 7 and 8, on the 3-year time scale, the NDVI change rate ranged from  $-0.96$  to  $0.62$ . The proportions of increasing and decreasing vegetation areas were 56.08% and 43.92%, respectively. This indicates that the vegetation change trend in the study area was mainly increasing, and 16.65% of the area showed a significant increasing trend, mainly distributed in the Shule River, Buha River, and Qinghai Nanshan in the west of the QLMs. However, the NDVI of the area significantly decreased by only 1.26% and was distributed sporadically in the Datonghe and Huangshui watersheds in the eastern and central parts of the QLMs.

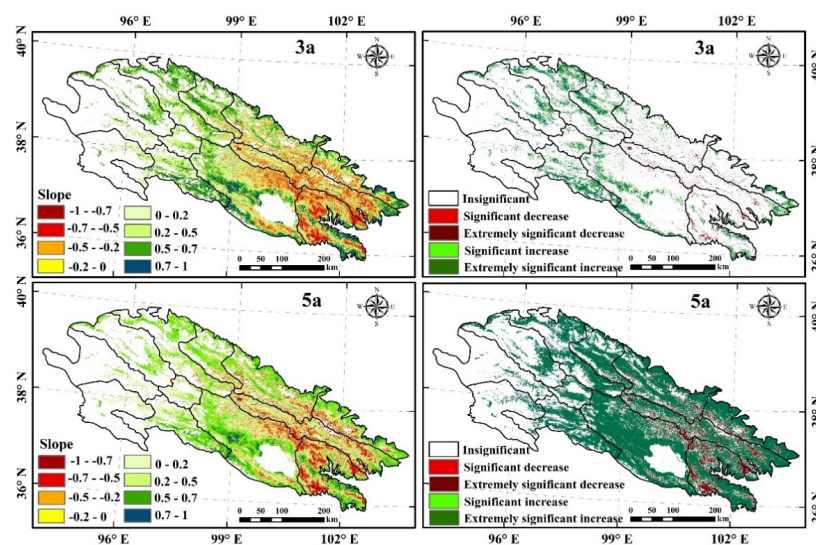
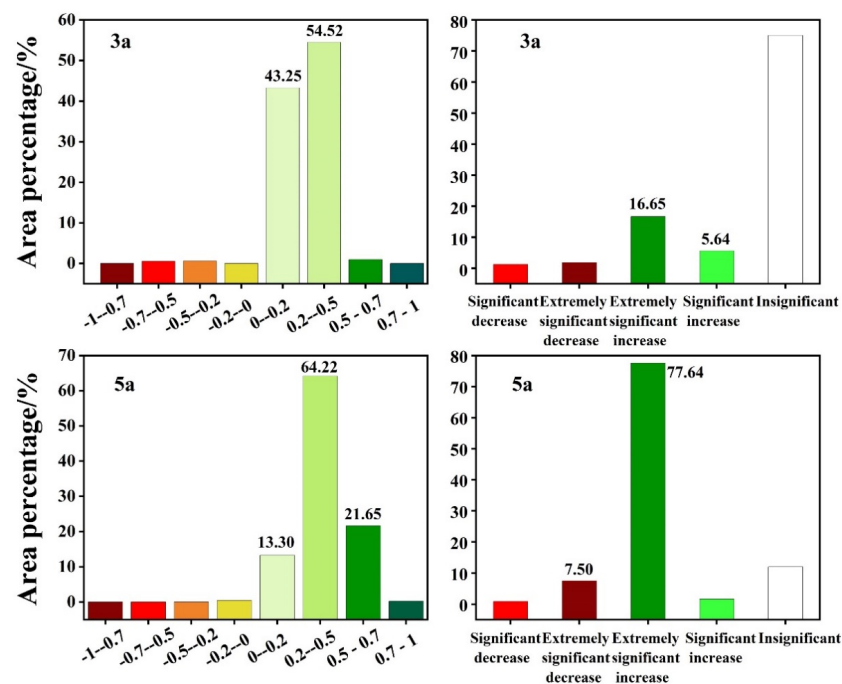


Figure 7. Spatial distribution of vegetation change at different time scales in the QLMs.



**Figure 8.** Statistical map of the area of change in the spatial distribution of vegetation at different time scales in the QLMs.

On the 5-year time scale, the NDVI change rate ranged from  $-0.97$  and  $0.96$ , and the proportions of increasing and decreasing areas were  $86.15\%$  and  $13.85\%$ , respectively. The NDVI showed a significant increasing trend in the whole study area. Compared with that on the 3-year time scale, the NDVI change rate on the 5-year time scale was larger and broader. The variation trend of NDVI values was more significant on the 5-year time scale. The area with an extremely significant increase trend was widely distributed in the western part of the study area, accounting for  $77.64\%$  of the total area. The area with an extremely significant decrease trend was much larger than that on the 3-year time scale, accounting for  $7.50\%$ , and distributed in the Datong River and Huangshui River basins. The long-term trend (Figure 5) showed that the NDVI values in the Shule River and Danghe River basins in the western part of the study area had an obvious increase trend, indicating that vegetations in these regions were dominated by a long-term trend. However, in the eastern and central regions, the negative vegetation change on the 5-year time scale was obvious, indicating that the vegetations in these regions mainly change in a 5-year cycle.

#### 4.3. Drivers of Vegetation Change in the QLMs

On the basis of the longitude, latitude, and altitude information of 16 meteorological stations in the QLMs, we used the Geodetector model to select eight factors as the driving factors: temperature (TEMPX1), LST (LSTX2), sunshine time (SUNTX3), precipitation (PREX4), ET (ETX5), relative humidity (HUMDX6), average wind speed (WINDX7), and DEM (DEMx8). We then conducted a factor detection analysis on the spatial distribution characteristics of vegetation and counted the  $q$  value of the driving factors (Figure 9a). To understand whether significant differences exist in the impacts of different factors on the spatial distribution of vegetation, we performed an ecological detection of the driving factors (Figure 9b).

The order of the  $Q$  value of the factor detector is as follows: SUNTX3 > WINDX7 > TEMPX1 > DEMx8 > LSTX2 > ETX5 > PREX4 > HUMDX6. This indicates that SUNT and WIND had the strongest explanatory power on the spatial distribution of vegetation in the QLMs, which were  $51.82\%$  and  $45.30\%$ , respectively. TEMP was the secondary factor (the explanatory power was  $34.11\%$ ). The influence of DEM (explanatory power,  $33.86\%$ ) on the spatial distribution of vegetation cannot be ignored. The effects of evapotranspiration, PRE,

and HUMD on the vegetation of the QLMs were relatively small, and their  $q$  values were at the same level. The explanatory power ranged from 10% to 20%, and the ecological test result was  $N$ . These indicate that the three had the same impact mechanism on the spatial distribution of vegetation and had no significant differences.

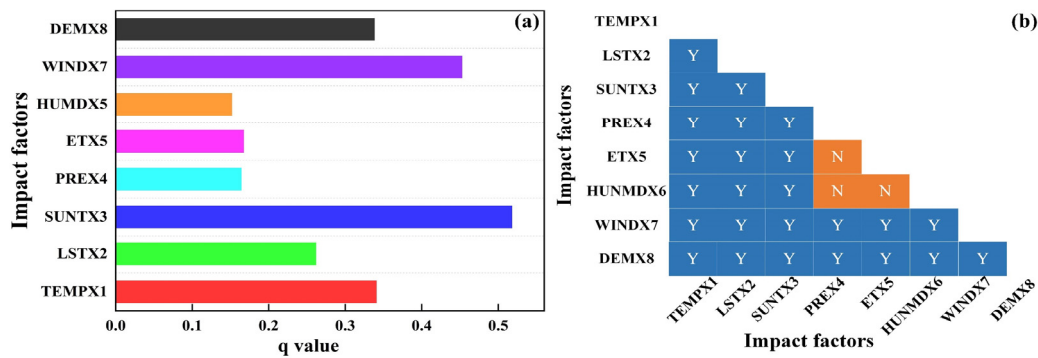


Figure 9. Factor detection (a) and ecological detection (b) results of the spatial distribution of vegetation.

In Figure 10, the change in colour from maroon (0.2–0.3) to dark blue (0.7–0.8) represents the changing process of the explanatory power of the interaction from low to high. The colour of the number represents the degree of explanatory power of the interaction. The size of the dot indicates the explanatory power of the two interaction factors more vividly and intuitively, and the two are unified. The interactive detection results (Figure 10) showed that when two driving factors simultaneously acted on the vegetation NDVI, the explanatory power of their interaction on the vegetation spatial distribution was greater than that of a single factor, which is basically enhanced by the two factors. The synergistic interactions between LST and SUNT (X2 and X3; explanatory power, 74.53%) and between HUMD and WIND (X6 and X7; 70.11%) were the most obvious, followed by those between TEMP and SUNT (69.93%), between TEMP and ET (69.69%), and between TEMP and PRE (69.43%). The interaction of temperature and other driving factors had greater explanatory power on the spatial distribution characteristics of vegetation. The interactive explanatory power of TEMP and PRE was significantly stronger than the single-factor explanatory power of the two driving factors. The explanatory power of PRE in factor detection was relatively weak but significantly enhanced in the interaction with altitude, indicating that the explanatory power of PRE on the spatial distribution of vegetation can be reflected only when a certain elevation is met [40]. The spatial distribution characteristics of vegetation are affected by not only one factor but also the result of the joint action of multiple factors.

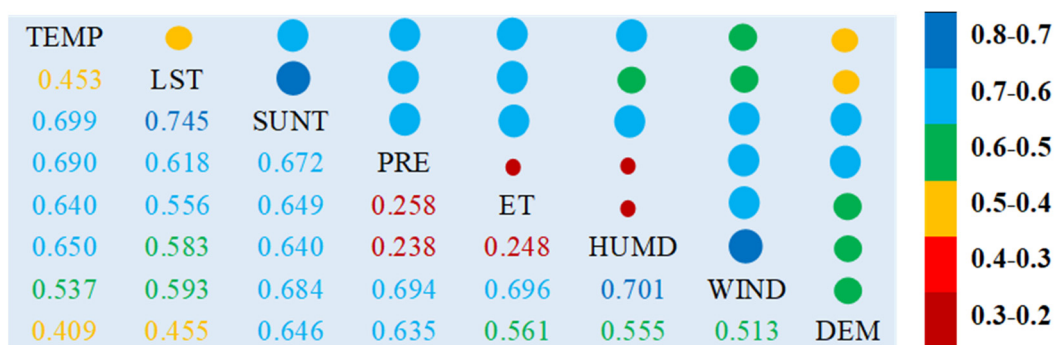
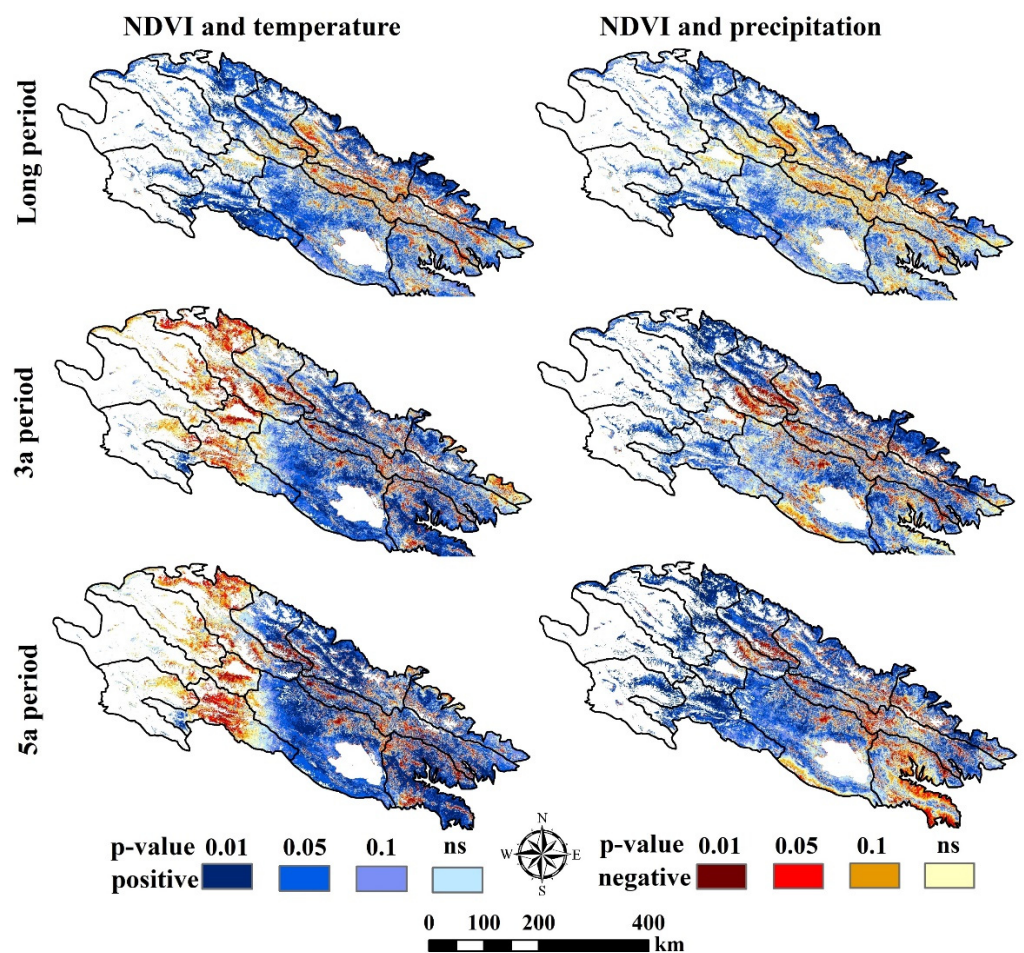


Figure 10. Interaction detection results for vegetation distribution in the QLMs.

#### 4.4. Correlation Analysis of Vegetation with Temperature and Precipitation in the QLMs

Although precipitation was relatively weakly explained in factor detection, precipitation was regional in nature, and somewhat influenced by elevation, which is particularly important in arid regions. Moreover, the interactive explanatory power of temperature and precipitation on the spatial variation of vegetation in the QLMs was significantly enhanced. Therefore, we chose to analyse the effects of single- and two-factor interactions between temperature and precipitation on vegetation at different time scales. As shown in Figure 11, the positive and negative correlation areas between vegetation and temperature were 67.18% and 32.82% on the 3-year scale, respectively. The correlation was not significant in most areas. The positive correlation was mainly distributed in the Bayingole River basin of Qinghai Lake in the south, the Beida River, and the Shule River basin in the north, accounting for around 7.86% ( $p < 0.05$ ). The negative correlation area was mainly distributed in the Huangshui, Datong, and Buha River basins in the east and middle of the study area, with a significant negative correlation of only 3.28%.



**Figure 11.** Spatial distribution of the correlation between vegetation and temperature and precipitation at different time scales.

On the 5-year time scale, the correlation between vegetation NDVI and temperature was significantly different, showing a spatial distribution state of positive correlation (40.23%) in the east and negative correlation (59.77%) in the west. The significant positive correlation was mainly concentrated in the Huangshui River and Shiyang River basins, accounting for 7.31% of the total area. The significant negative correlation was mainly distributed in the Shule River, Danghe River, and Bayingole River basin. In the long-term trend, the areas of positive and negative correlations between vegetation and temperature

were similar, at 43.18% and 54.12%, respectively. Around 51.56% of the vegetation in the study area had a significant correlation with temperature, of which 18.01% had a significant positive correlation, and was mainly distributed in the Laji Mountain, Qinghai Lake, Shiyang River, and Beidahe River basins. The significant negative correlation was mainly distributed in the west of the Datong River Basin, Buha River, and Bayingole River.

The long-term warming trend has a certain inhibitory effect on vegetation growth in these basins. On the 3-year time scale, vegetation and precipitation mainly positively correlated, and the spatial distribution was similar to the correlation distribution of vegetation temperature. The positive correlation and negative correlations accounted for 58.73% and 41.27% of the study area, respectively, but were not significant. On the 5-year time scale, the correlation between vegetation NDVI and precipitation was not significant, and the overall significance level was lower than 0.1. Under the long-term change trend, the correlation between vegetation and precipitation showed obvious spatial differences. The positive correlation was mainly distributed in the east of the study area, accounting for 56.66%. Of this, the extremely significant positive correlation accounted for 9.83% ( $p < 0.01$ ), which was mainly concentrated in Henan of Datong and Hubei of Qinghai. The negative correlation was mainly distributed in the northwest of the study area. The vegetation in the arid area of the west was more sensitive to water change and had a greater demand for precipitation. However, the correlation results showed that vegetation in the west mainly negatively correlated with precipitation. The main reason may be that the different vegetation types have different demands for precipitation or may be related to the lag between them [16].

Obviously, vegetation change in the QLMs was jointly affected by temperature and precipitation, and the degrees of response of different regions to temperature and precipitation were different. To further understand the main driving force of vegetation change in different regions, this study reclassified the  $P$  values of the correlations of NDVI with temperature and precipitation. When the correlation coefficient  $p$  between NDVI and temperature was less than 0.05 and the correlation coefficient  $p$  between NDVI and precipitation was greater than 0.05, temperature was considered the main driving force; otherwise, it was precipitation. When the correlation coefficient  $p$  between NDVI and temperature or between NDVI and precipitation was less than 0.05, we inferred that the vegetation change was the result of the joint action of temperature and precipitation. However, when both  $p$  values were greater than 0.05, vegetation growth was presumed to have little correlation with the variables.

From Figure 12, under the long-term trend, around 24.43% of the regional vegetation change in the study area was mainly driven by precipitation, which was mainly distributed in the northern and southern marginal basins of the Shule River, Heihe River, and Bayingole River. The main driving force of around 7.79% of the regional vegetation change was temperature, which was distributed in the Huangshui and Datong River basins. On the 3-year time scale, the driving effect of temperature on vegetation growth was significantly enhanced. The main driving force of vegetation change in the Huangshui and Qinghai Lake basins in the East was temperature, covering an area of 17.40 km<sup>2</sup>. The driving force of vegetation change in the entire study area was still precipitation, accounting for around 26.81%. In the middle of the Chase River, the joint effects of temperature and precipitation were obvious, accounting for approximately 9.02%. On the 5-year time scale, temperature was the main driving force, and the area under the joint action of temperature and precipitation further increased by 11.46%, especially in the Buha River, Heihe River, and Datong River Basin.

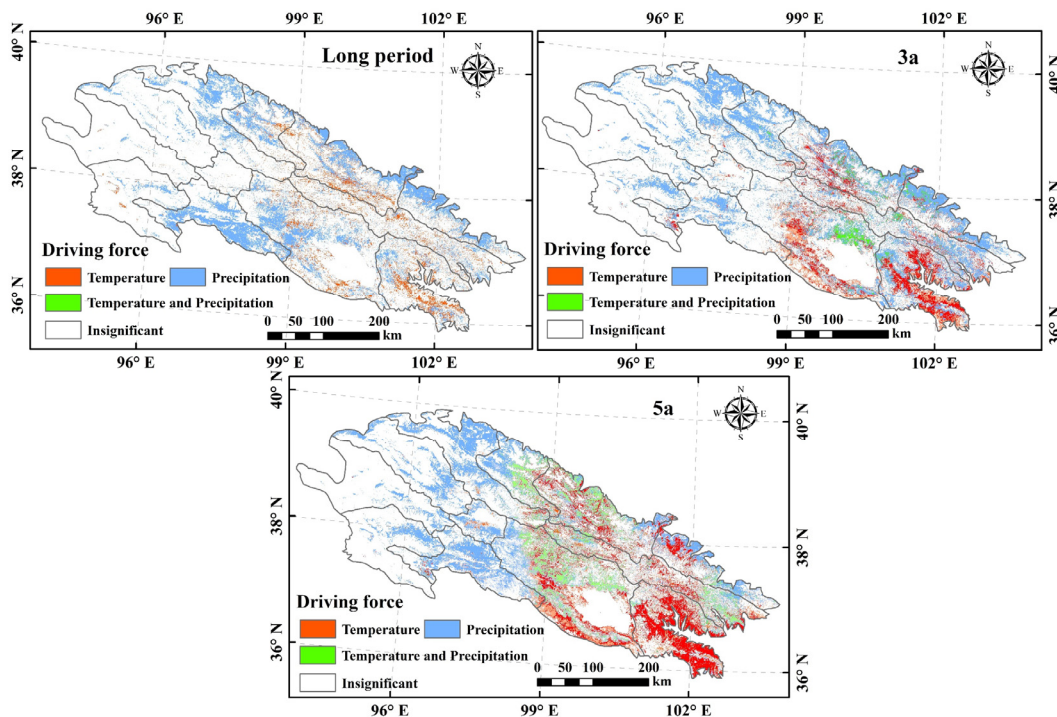


**Figure 12.** Main drivers of vegetation change at different time scales.

## 5. Discussion

### 5.1. Characteristics of Vegetation Change in the QLMs

The QLMs, located at the junction of Mengxin, Qinghai-Tibet, and Loess Plateau, are a case in an ecologically fragile area in northwest China. Vegetation plays an important role in maintaining regional ecological balance. Changes in large-scale vegetation coverage can reflect the impact of natural and human activities on the ecological environment [41]. On the other hand, vegetation plays an irreplaceable role in maintaining regional ecological balance, especially in reducing soil erosion. In recent years, under the influence of global warming, vegetation in the QLMs has undergone significant changes, showing an upward trend year after year [42]. This study confirms the previous report that the vegetation NDVI in the QLMs has shown a fluctuating upward trend in recent decades (Figure 3). Westerly wind prevails in the central and western parts of the QLMs all year round, while marine monsoons affect the eastern part. The different moisture sources in the eastern and western parts cause an increasing trend of precipitation in the QLMs from west to east [43]. This is an important factor that leads to the pattern of more vegetation in the eastern part and less vegetation in the western part (Figure 4).

From 2000 to 2019, the vegetation in the QLMs showed an improvement trend (Figure 5). The improvement in overall vegetation coverage depends on the growth of local vegetation NDVI [44]. The EEMD decomposition results of vegetation NDVI showed that the vegetation in the QLMs had a significant cycle and long-term increase trend in the 3- and 5-year projections (Figure 6). The NDVI changes were most significant on the 3-year time scale and over the long-term trends (Figures 7 and 8), indicating that the vegetation dynamics in the QLMs were mainly characterised by 3-year fluctuations and showed a continuous increase trend, which was consistent with the time scale of the vegetation NPP change in northwest China [35].

The implementation of a series of national and local government ecological projects and policies in recent years may be the main reason for the obvious improvement of vegetation in the human activity area of the QLMs. For example, the implementation of the policy of herdsmen moving to the valley area helps reduce grazing pressure in the study area and promotes the development of vegetation in a good direction [45,46]. Human

activities such as urbanisation, water diversion projects, and overgrazing have adverse effects on vegetation in human activity areas. On the other hand, the implementation of measures such as rectifying mining, hydropower and tourism projects, rotational grazing, and grazing withdrawal, to a certain extent, promoted the restoration of vegetation. Overall, the vegetation in the QLMs has improved significantly since 2017. Most of the vegetation types that showed increases are mixed forests for ecological protection and restoration, indicating that the implementation of vegetation restoration and ecological protection policies in the QLMs has positive effects on vegetation improvement.

### 5.2. Analysis of the Driving Forces of Vegetation Change in the QLMs

Environmental factors such as TEMP, PRE, LST, DEM, ET, WIND, and SUNT were important driving factors for the temporal and spatial evolutions of the NDVI in the QLMs (Figure 9). SUNT and WIND were the primary factors that affected the spatial distribution of vegetation in the QLMs, followed by TEMP, DEM, LST, and ET. PRE and HUMD ranked lower in the explanatory power of geographical exploration. This study shows that WIND and SUNT were important factors that affected the growth of desert vegetation. The increase in WIND was not conducive to the growth of desert vegetation, while SUNT directly affected the photosynthetic efficiency and productivity of vegetation. WIND and SUNT have non-negligible impacts on the spatial distribution of vegetation in the QLMs [47].

In a humid environment, where water supply is enough for vegetation growth, a change in temperature will directly affect the transpiration and chlorophyll synthesis of plants. Therefore, temperatures in the Huangshui, Heihe, Datong, and Shiyang River basins in the east have become the dominant factor affecting the spatial distribution of vegetation. This corresponds to the existing research conclusions that the impact of temperature change on the spatial distribution of vegetation will be amplified and the feedback of vegetation spatial distribution will also become larger in a humid environment [48]. Sufficient water conditions are necessary for the growth of desert vegetation. However, different hydrothermal conditions also create varied vegetation growth habits. In recent years, much glacial melt water caused by climate warming has provided sufficient water conditions for the growth of vegetation in the QLMs [49,50].

In the past few decades, vegetation NDVI change had had a good correlation with precipitation and evapotranspiration [51]. Vegetation cover change has a significant correlation with surface temperature [52]. A previous study showed that the explanatory power of precipitation on the spatial distribution of vegetation increased under specific altitude conditions [46]. The explanatory powers of temperature and precipitation on the spatial distribution of vegetation in the west of the study area were stronger than those in the east, and the interactive interpretation is large (Figure 10). Furthermore, the spatial explanatory power of altitude to vegetation may be related to the regional scope. On the one hand, the vegetation degradation area of the QLMs is related to the reduction of precipitation in the region. In low-altitude areas, human activities such as overgrazing and farmland reclamation cause land desertification and lead to vegetation degradation [53].

The correlations of vegetation NDVI to temperature and precipitation in the QLMs were significantly different (Figures 11 and 12). On a 3-year time scale, the increase in temperature and precipitation promoted vegetation growth in the Qinghai Lake basin. The short-term temperature increase was conducive to the increase of vegetation in the Shule River and Beidahe River basins in the northwest. In the long term, the increase in temperature and precipitation was conducive to the study of the growth of vegetation in the east. The increase in temperature hindered the increase in vegetation in the central part, and the increase in precipitation was not conducive to the growth of vegetation in some western areas. These may be due to the increase in temperature and surface evapotranspiration and the decrease in available water for vegetation growth [47]. In the short term, the increase in temperature was not conducive to the growth of vegetation in the western arid area, which is consistent with the driving force detection results of the main

controlling factors in the study area. In the long-term series, the correlation analysis results in the western part of the study area showed a negative correlation between precipitation and vegetation. This contradicts the driving force detection results of the main controlling factors of precipitation in the spatial distribution of vegetation in the western part of the study area.

By studying and analysing the relevant data on vegetation and precipitation in recent decades, we found a 1-year difference in the significant cycle of vegetation and precipitation, which is consistent with the lag problem of vegetation response to precipitation change. Therefore, we inferred that the lag in precipitation and vegetation may be the main reason for the negative correlation between precipitation and vegetation in the west [16,54]. In summary, in the long-term trend and on the short-term scale, precipitation was the main driving force for vegetation growth in the north and southwest of the QLMs. Short-term temperature changes had a great impact on vegetation in the east. On the 5-year time scale, the vegetation changes in most areas of the study area were mainly driven by temperature and precipitation, and the interaction between the vegetation dynamics will lead to the potential feedback of the vegetation climate system.

### 5.3. Limitations and Future Perspectives

This study provides an in-depth study of the characteristics and driving factors of the vegetation change in the QLMs based on multiple time scales. However, satellite data are often affected by the uncertainty of noise and system errors, and these uncertainties are often not fully quantified with precision to circumvent. Although the multi-sensor NDVI dataset has been widely used in local and global modelling and analysis, many previous studies have shown considerable deviations in NDVI records between different sensors. The accuracy of NDVI time series data is limited. Thus, we propose introducing higher-precision and longer time series data in studies and analyses to improve the overall quality of results in future research. The analysis of the impact of human activities, the main research data from the existing literature, failed to combine the specific characteristics of human activity data in the quantitative research on vegetation change in the QLMs. We propose studying the driving forces of vegetation change in greater depth in future studies by combining information from data related to anthropogenic activities, such as population, economy, and land cover change.

## 6. Conclusions

Herein, we studied the spatial and temporal variations and cyclical characteristics of vegetation in the QLMs on the basis of MODIS NDVI data from 2000 to 2019 and GIMMS NDVI data from 1982 to 2006 of the QLMs. From these data, we combined various meteorological data, DEM, LST, and ET, and the linear trend method, EEMD, Geodetector, and correlation analysis to examine the main drivers of vegetation change and analyse the effects of temperature and precipitation on vegetation. The main conclusions are as follows:

- (1) The overall vegetation in the QLMs showed an increasing trend. The vegetation in the QLMs showed high northeast and low southwest distributions in 2000–2019, with slight decreases in the east and central parts and a significant increase in the northwest. The vegetation in the entire study area had 3- and 5-year cycles of change and a long-term increasing trend. On the short time scales, the vegetations in the central and eastern parts of the study area were influenced more by non-climatic factors such as human activities, whereas in long-term trends, the vegetation was mainly influenced by climatic factors.
- (2) The  $q$  values of the Geodetector results were ranked as follows: SUNT > WIND > TEMP > DEM > LST > ET > PRE > HUMD. SUNT and WIND had the strongest explanatory power for the spatial variation of vegetation in the QLMs. The explanatory powers of TEMP and PRE for the spatial variation of vegetation were greater and increased under certain elevation conditions, respectively. The explanatory powers of

TEMP and PRE on the spatial variation of vegetation in the western part of the study area were greater than those in the eastern part, and the explanatory power of the interaction was greater.

- (3) Precipitation was the main driver of vegetation growth in the northern and south-western regions of the QLMs on both the short and long time scales. The increases in temperature and precipitation contributed to the vegetation growth in the Qinghai Lake basin on the 3-year time scale. Short-term temperature increases contributed to the increase in vegetation in the northwestern area of the QLMs. By contrast, a long-term trend of combined increases in temperature and precipitation favoured the growth of vegetation in the eastern part of the study area.

**Author Contributions:** Conceptualization, L.Z. and H.Y.; methodology, Y.H.; software, L.Q.; validation, L.Z., H.Y. and Y.H.; formal analysis, L.Q.; data curation, G.P.; writing—original draft preparation, L.Z.; writing—review and editing, Y.H.; visualization, S.C.; funding acquisition, L.Z. All authors have read and agreed to the published version of the manuscript.

**Funding:** This research was funded by the National Scientific Foundation of China (Grants Nos. 42161063), LZJTU EP, No201806, Natural Science Foundation of Gansu Province (20JR10RA249), Youth Science and Technology Foundation of Gansu Province (20JR10RA272), and Tianyou innovation team of Lanzhou Jiaotong University (TY202001).

**Institutional Review Board Statement:** Not applicable.

**Informed Consent Statement:** Not applicable.

**Data Availability Statement:** The data presented in this study are available on request from the corresponding author. The data are not publicly available due to privacy.

**Conflicts of Interest:** The authors declare no conflict of interest.

## References

- Li, X.; Li, X.B.; Wang, H.; Yu, F.; Yu, H.J.; Yang, H. Impact of climate change on temperate grassland in northern China. *J. Beijing Norm. Univ. Nat. Sci.* **2006**, *42*, 623–818.
- Song, Y.; Jin, L.; Wang, H. Vegetation Changes along the Qinghai-Tibet Plateau Engineering Corridor Since 2000 Induced by Climate Change and Human Activities. *Remote Sens.* **2018**, *10*, 95. [[CrossRef](#)]
- Deng, X.Y.; Yao, J.Q.; Liu, Z.H. Spatiotemporal dynamic change of vegetation coverage in central Asia based on GIMMS NDVI. *Arid Zone Res.* **2017**, *1*, 10–19.
- Chen, J.H.; Jia, W.X.; Zhao, Z.; Zhang, Y.S.; Liu, Y.R. Research on temporal and spatial variation characteristic of vegetation cover of Qilian Mountains from 1982 to 2006. *Adv. Earth Sci.* **2015**, *30*, 834–845.
- Duo, A.; Zhao, W.J.; Gong, Z.N.; Zhang, M.; Fan, Y.B. Temporal analysis of climate change and its relationship with vegetation cover on the north China plain from 1981 to 2013. *Acta Ecol. Sin.* **2017**, *37*, 576–592.
- Xie, B.N. *Vegetation Dynamics and Climate Change on the Loess Plateau, China: 1982–2014*; Northwest A & F University: Xianyang, China, 2016.
- Chao, Y.S. *Principles and Methods of Remote Sensing Application Analysis*; Science Press: Beijing, China, 2003.
- Pu, S.L.; Fang, J.Y. Seasonal differences in response of land vegetation activities to climate change in China from 1982 to 1999. *Acta Geogr. Sin.* **2003**, *58*, 119–125.
- Cao, M.; Woodward, F.L. Dynamic responses of terrestrial ecosystem carbon cycling to global climate change. *Nature* **1998**, *393*, 249–252. [[CrossRef](#)]
- Liu, M.X.; Zhao, R.D.; Shao, P. Temporal and spatial variation of vegetation coverage and its driving forces in the Loess Plateau from 2001 to 2015. *Arid Land Geogr.* **2018**, *41*, 99–108.
- Zhang, L.J.; Zhang, B.Y.; Li, W.L.; Li, X.X.; Sun, L.; Jiang, L.J.; Liu, X.X. Spatiotemporal changes and drivers of global land vegetation oxygen production between 2001 and 2010. *Ecol. Indic. Integr. Monit. Assess. Manag.* **2018**, *90*, 426–437. [[CrossRef](#)]
- Pan, N.Q.; Feng, X.M.; Fu, B.J.; Wang, S.; Pan, S.F. Increasing global vegetation browning hidden in overall vegetation greening: Insights from time-varying trends. *Remote Sens. Environ.* **2018**, *214*, 59–72. [[CrossRef](#)]
- Li, X.F.; Zhu, X.F.; Li, S.S.; Liu, Y.X.; Pan, Y.Z. Changes in Growing Season Vegetation and Their Associated Driving Forces in China during 2001–2012. *Remote Sens.* **2015**, *7*, 15517–15535. [[CrossRef](#)]
- Li, J.; Liu, H.B.; Li, C.Y.; Li, L. Changes of green-up day of vegetation season based on GIMMS 3g NDVI in northern China in recent 30 years. *Sci. Geogr. Sin.* **2017**, *37*, 143–152.
- Dai, S.P.; Zhang, B.; Wang, H.J.; Wang, Y.M.; Li, D.; Wang, X.M. Analysis on the spatio-temporal variation of grassland cover using SPOT NDVI in Qilian Mountains. *Prog. Geogr.* **2010**, *29*, 1075–1080.

16. Wu, Z.L.; Jia, W.X.; Zhao, Z.; Zhang, S.Y.; Liu, Y.R.; Chen, J.H. Spatial-temporal variations of vegetation and its correlation with climatic factors in Qilian Mountains from 2000 to 2012. *Arid Land Geogr.* **2015**, *38*, 1241–1252.
17. Xu, X.; Liu, H.; Lin, Z.; Jiao, F.; Gong, H. Relationship of Abrupt Vegetation Change to Climate Change and Ecological Engineering with Multi-Timescale Analysis in the Karst Region, Southwest China. *Remote Sens.* **2019**, *11*, 1564. [[CrossRef](#)]
18. Xu, G.; Zhang, H.; Chen, B.; Zhang, H.; Innes, J.L.; Wang, G.; Yan, J.; Zheng, Y.; Zhu, Z.; Myneni, R.B. Changes in Vegetation Growth Dynamics and Relations with Climate over China's Landmass from 1982 to 2011. *Remote Sens.* **2014**, *6*, 3263–3283. [[CrossRef](#)]
19. Jung, M.; Reichstein, M.; Bondeau, A. Towards global empirical upscaling of FLUXNET eddy covariance observations: Validation of a model tree ensemble approach using a biosphere model. *Biogeosciences* **2009**, *6*, 2001–2013. [[CrossRef](#)]
20. Meng, X.; Gao, X.; Li, S.; Lei, J. Spatial and Temporal Characteristics of Vegetation NDVI Changes and the Driving Forces in Mongolia during 1982–2015. *Remote Sens.* **2020**, *12*, 603. [[CrossRef](#)]
21. Wang, W.H.; He, Y.; Zhang, L.F.; Chen, Y.D.; Tang, Y.W.; Qiu, L.S.; Zhang, X.X. Ground deformation monitoring and driving force analysis of the main city area in Lanzhou based on PS-InSAR and GeoDetector. *J. Lanzhou Univ. Nat. Sci. Ed.* **2021**, *57*, 382–388.
22. He, Y.; Wang, W.; Chen, Y.; Yan, H. Assessing spatio-temporal patterns and driving force of ecosystem service value in the main urban area of guangzhou. *Sci. Rep.* **2021**, *11*, 3027. [[CrossRef](#)]
23. Liu, Y.R.; Jia, W.X.; Huang, M.; Li, Y.Y.; Wu, Z.L.; Zhang, S.Y.; Li, Y.F. Response of vegetation net primary productivity to climate in the Qilian Mountains since recent 51 years. *Acta Bot. Boreal. Occident. Sin.* **2015**, *35*, 0601–0607.
24. Zhao, S.M.; Cheng, W.M.; Zhou, C.H.; Chen, X.; Chen, J. Simulation of decadal alpine permafrost distributions in the Qilian Mountains over past 50 years by using Logistic Regression Model. *Cold Reg. Sci. Technol.* **2012**, *73*, 32–40. [[CrossRef](#)]
25. Dong, L. *The Freezing Level Height and Its Impact Variation of Water Resource in Qilian Mountains during 1979–2012*; Northwest Normal University: Lanzhou, China, 2015.
26. Zhang, F.G.; Zeng, B.; Yang, T.B. Spatiotemporal distribution changes in alpine desert belt in Qilian Mountains under climate changes in past 30 years. *Chin. J. Plant Ecol.* **2019**, *43*, 305. [[CrossRef](#)]
27. Yu, M.; Cao, G.C.; Cao, S.K.; Zhang, H.; Yuan, J. Analysis of precipitation variation characteristics in the southern slope of Qilian Mountains in recent 30 years. *Res. Soil Water Conserv.* **2019**, *26*, 245–252.
28. Jin, B.W.; Kang, E.S.; Song, K.C. Eco-hydrological function of mountain vegetation in the Hei River Basin, northwest China. *J. Glaciol. Geocryol.* **2003**, *25*, 580–584.
29. Wang, Q.; Zhang, B.; Dai, S.P. Analysis of the vegetation cover change and its relationship with factors in the Three-North Shelter Forest Program. *China Environ. Sci.* **2012**, *32*, 1302–1308.
30. Bi, C. *Dynamics of Vegetation and Phenology and Their Response to Climate Change Based on Multisource Data in the Arid and Semiarid Region, China*; Beijing Forestry University: Beijing, China, 2015.
31. Zeng, B. *Vegetation Responses to Climate Change on the Tibetan Plateau 1982–2003*; Lanzhou University: Lanzhou, China, 2008.
32. Felix, N.; Hao, G.; Anming, B. Understanding the Spatial Temporal Vegetation Dynamics in Rwanda. *Remote Sens.* **2016**, *8*, 129.
33. Zhang, L.F.; Yan, H.W.; Yang, S.W.; Zhu, J.W.; Qiu, L.S. Variations of vegetation coverage and its response to terrain in Heihe River Basin. *Remote Sens. Inf.* **2018**, *33*, 46–52.
34. Li, E.S.; Zhou, X.M.; Zhang, B.M. Study on the image noises elimination based on the wavelet transform and gauss function. *Mar. Geod. Cartogr.* **2008**, *28*, 41–44.
35. Jia, J.H.; Liu, H.Y.; Lin, Z.S. Multi-time scale changes of vegetation NPP in six provinces of northwest China and their responses to climate change. *Acta Ecol. Sin.* **2018**, *39*, 5058–5069.
36. Tang, L.; Zhao, Z.M.; Tang, P. A new method for detection “greening” or “browning” change trend in vegetation from NDVI sequences. *Remote Sens. Land Resour.* **2019**, *31*, 89–95.
37. Tao, Y.; Liu, C.; Liu, C.; Zhao, X.W.; Hu, H.J. Empirical Wavelet Transform Method for GNSS Coordinate Series Denoising. *J. Geovis. Spat. Anal.* **2021**, *5*, 9. [[CrossRef](#)]
38. Wang, J.F.; Xu, C.D. Geodetector: Principle and prospective. *Acta Geogr. Sin.* **2017**, *72*, 116–134.
39. He, Y.; Yan, H.W.; Ma, L.; Zhang, L.F.; Qiu, L.S.; Yang, S.W. Spatiotemporal dynamics analysis of vegetation in Ningxia of China using MODIS imagery. *Front. Earth Sci.* **2020**, *14*, 221–235. [[CrossRef](#)]
40. Pei, Z.L.; Yang, Q.K.; Wang, C.M.; Pang, G.W.; Yang, L.H. Spatial distribution of vegetation coverage and its affecting factors in the upper reaches of the Yellow River. *Arid Zone Res.* **2019**, *3*, 546–555.
41. Liu, H.Y.; Zhang, M.Y.; Lin, Z.S.; Xu, X.J. Spatial heterogeneity of the relationship between vegetation dynamics and climate change and their driving forces at multiple time scales in Southwest China. *Agric. For. Meteorol.* **2018**, *256*, 10–21. [[CrossRef](#)]
42. Yao, Z.Y.; Zhao, C.Y.; Yang, K.S.; Liu, W.C.; Li, Y.; You, J.D.; Xiao, J.H. Alpine grassland degradation in the Qilian Mountains, China—a case study in Damaying grassland. *Catena* **2016**, *137*, 494–500. [[CrossRef](#)]
43. Chen, Y.; Xu, D.X.; Guo, N. Analysis on the vegetation change in Qilian Mountains since recent 22 years. *Arid Zone Res.* **2008**, *6*, 22–27.
44. Zhang, Y.; Xu, G.; Li, P.; Li, Z.; Wang, Y.; Wang, B.; Jia, L.; Cheng, Y.; Zhang, J.; Zhuang, S.; et al. Vegetation Change and Its Relationship with Climate Factors and Elevation on the Tibetan Plateau. *Int. J. Environ. Res. Public Health* **2019**, *16*, 4709. [[CrossRef](#)]
45. Qiu, L.S.; Zhang, L.F.; He, Y.; Diao, Z.Y.; Chen, Y.D. Remote sensing monitoring on vegetation dynamic change in Qilian Mountain from 2000 to 2017. *Remote Sens. Inf.* **2019**, *34*, 97–107.

46. Geng, L.; Che, T.; Wang, X.; Wang, H. Detecting Spatiotemporal Changes in Vegetation with the BFAST Model in the Qilian Mountain Region during 2000–2017. *Remote Sens.* **2019**, *11*, 103. [[CrossRef](#)]
47. Qiu, L.S. *Study on Multiscale Variation Characteristics of Vegetation and Driving Forces in Qilian Mountains*; Lanzhou Jiaotong University: Lanzhou, China, 2020.
48. Niu, Z.G.; He, H.L.; Zhu, G.F.; Ren, X.L.; Zhang, L.; Zhang, K.; Yu, G.R.; Ge, R.; Li, P.; Zeng, N. An increasing trend in the ratio of transpiration to total terrestrial evapotranspiration in China from 1982 to 2015 caused by greening and warming. *Agric. For. Meteorol.* **2019**, *279*, 107701. [[CrossRef](#)]
49. Wang, J.F. Analysis on runoff variation in the Beida River Basin under the influence of climate change and human activities. *J. Arid Land Resour. Environ.* **2019**, *33*, 88–93.
50. Cheng, Y.S.; Cheng, Z.J. Studies on relationship between runoff characteristics of Danghe River Basin and climate change in recent 40 years. *China Water Resour.* **2015**, *13*, 60–63.
51. Zhao, X.; Tan, K.; Zhao, S.; Fang, J. Changing climate affects vegetation growth in the arid region of the northwestern China. *J. Arid Environ.* **2011**, *75*, 946–952. [[CrossRef](#)]
52. Wang, M.N.; Han, Z.; Zhang, Q.Y. Impact of land use and cover change in the semi-arid regions of China on the temperature in the early 21st century. *Clim. Environ. Res.* **2016**, *21*, 65–77.
53. Jiang, Y.Y.; Du, W.T.; Huang, J.; Zhao, H.Z.; Wang, C.F. Analysis of vegetation changes in the Qilian Mountains during 2000–2015. *J. Glaciol. Geocryol.* **2017**, *39*, 1130–1136.
54. Jia, W.X.; Chen, J.H. Variations of NDVI and its response to climate change in the growing season of vegetation in Qilian Mountains from 1982 to 2014. *Res. Soil Water Conserv.* **2018**, *25*, 264–268.